

IN THE UNITED STATES PATENT AND TRADEMARK OFFICE

**APPLICATION FOR LETTERS PATENT**

\* \* \* \* \*

**METHOD FOR PREDICTING DYNAMIC  
PARAMETERS OF FLUIDS  
IN A SUBTERRANEAN RESERVOIR**

\* \* \* \* \*

**INVENTORS**

**VLADIMIR B. PISETSKI  
VALERI V. KORMILCEV  
and  
ALEKSANDER N. RATUSHNAK**

ATTORNEY'S DOCKET NO. TR01-P04

1                   **METHOD FOR PREDICTING DYNAMIC PARAMETERS OF FLUIDS**  
2                   **IN A SUBTERRANEAN RESERVOIR**

3                   **CROSS REFERENCE TO RELATED APPLICATION**

4                   This application is a Continuation in Part of U.S. Patent Application Serial Number  
5                   09/134,616, filed August 14, 1998, <sup>now US Pat. # 6,028,820</sup> which is a Continuation in Part of U.S. Patent Application  
6                   Serial Number 08/909,454, filed August 11, 1997, now U.S. Patent No. 5,796,678, issued August  
7                   18, 1998.

8

9                   **FIELD OF INVENTION**

10                  This invention pertains to a method for predicting the dynamic parameters of fluids in a  
11                  subterranean reservoir.

12

13                  **BACKGROUND OF THE INVENTION**

14                  In the search for subterranean fluids (typically natural gas and/or petroleum), classical  
15                  methods have used seismic imaging to generate an image of a subterranean region of exploration.  
16                  Modern three dimensional (3D) seismic imaging has aided a great deal in developing credible  
17                  models of the region of interest. Information regarding travel time of seismic signals can be used to  
18                  estimate velocities of various subsurface layers, which provides information indicative of the rock  
19                  type. Hydrocarbons are often trapped by geologic faults, and so the seismic images are  
20                  subsequently interpreted to identify rock types which, in conjunction with geologic faults or other  
21                  phenomenon, would result in an accumulation of fluids in an area in the region of study. However  
22                  seismic information provides only limited information. Unless the geologic fault has a seal, fluids  
23                  will not be trapped. Unfortunately, seismic survey data does not contain sufficient information to  
24                  indicate the presence or absence of a seal. Other information is desirable which, if used in

1 conjunction with seismic images, would improve the probability of finding hydrocarbons.

2 It is known that the field of so-called prestresses in the earth's crust is determined by two  
3 systems of external forces, namely, gravitational and tectonic forces. The joint action of these forces  
4 can result in compaction as well as in unloading of rock masses with respect to their normal  
5 gravitational or lithostatic stress condition. The existing theory describing stress fields in the earth's  
6 crust is absolutely correct for elastic and continuous media. At the same time information derived  
7 from a number of wells, drilled down to 10 km, points to the presence of fractures in sedimentary  
8 and crystalline parts of the earth's crust. Since there is little reason to expect presence of spatially  
9 localized fractures, we can affirm that any real rock unit is bounded by a closed system of fractures  
10 and represents a discrete system. Taking into account a well-known concept that any basin  
11 represents a tectonically young and consequently active structure, these are all reasons to consider  
12 any unit of the sedimentary cover as a part of discrete dynamic system. To date, no one has thought  
13 to use information pertaining to stress in the earth's crust as part of a method for determining the  
14 presence of fluid in a subterranean formation. Our invention uses seismic imaging information in  
15 conjunction with formation stress information to improve the reliability of seismic exploration for  
16 hydrocarbons.

17 The publication of J. D. Byerlee ("Friction of Rocks", *Pure Applied Geophysics*, 116  
18 (1978), pp. 615-626) is useful for estimating parameters of stress condition of fractured and discrete  
19 rock units. He has found that the maximum differential stress (the difference of main stresses) in the  
20 upper part of the earth's crust is limited by the shear strength of fractured rocks. Laboratory  
21 investigations show that the sliding friction on the surface of fractured rocks exists until the external  
22 load reaches the critical value of brittle failure. At the same time the strength of such a discrete  
23 rock unit is determined by cohesion of fractures on its surface and does not practically depend on  
24 the elastic moduli of the rock, temperature, strain value, and the type of sliding surface. It is

1 determined that the cohesive force  $\tau$  is a linear function of normal load  $\sigma_n$  (Byerlee's law):

2  $\tau = 0.85 \sigma_n$   $3 < \sigma_n < 200 \text{ MPa}$  (1)

3 or in the terms of main stresses, the limit value of horizontal stresses down to the depths of 5 km

4 is estimated to be

5  $\sigma_1 \approx 5\sigma_3$   $\sigma_3 < 110 \text{ MPa}$  (2)

6 In other words the main component of stress condition variation in discrete media is  
7 associated with the change of vertical load. Insignificant movement in the base of a sedimentary  
8 basin (for example, in the crystalline basement) results in considerable change of the horizontal  
9 component of stress. The strength limit of a rock unit is rapidly reached, and all the sedimentary  
10 cover is set in motion continuously approaching the isostatic equilibrium. Thus, it is reasonable to  
11 suggest that real sedimentary formations have a high degree of mobility in vertical direction. As  
12 time of stress relaxation characteristic for discrete media is significant, the stress distribution in the  
13 basin has distinctive contrasting character and is governed by the principles of block dynamics.

14 The most fundamental theoretical results in the field of elastic wave propagation in  
15 prestressed media were derived by M. A. Biot (textbook, *Mechanics of Incremental Deformations*,  
16 New York, 1965). Biot introduced a new type of strain, strain of solid rotation. Its introduction is  
17 related to non-hydrostatic character of prestress field in the medium (i.e. horizontal and vertical  
18 components of the stress field are not equal to each other). In this case each unit volume of the  
19 medium has been rotated through some angle with respect to its initial position in the unstressed  
20 medium. As a result additional strains appear in the wave field, and their amplitudes are directly  
21 proportional to the difference between horizontal and vertical components of the prestress field ( $\sigma_1$   
22 и  $\sigma_3$ ). A number of researchers studied the equations derived by M. A. Biot and came to the  
23 conclusion that the influence of initial stresses on traveltimes and, especially, amplitude parameters

1 of seismic waves, can be very significant, and the degree of this influence is proportional to the  
2 ratio  $P/\mu$  (where  $P$  is pressure and  $\mu$  is the shear modulus).

3 A significant number of publications are related to investigation of the stress condition of  
4 the earth with the aid of seismic methods. But practically all these investigations were based on the  
5 analysis of traveltimes parameters and were reduced to attempts to explain complex distribution of  
6 velocity parameters by the influence of lithostatic pressure. In this case the stress condition of the  
7 subsurface is taken into account indirectly using theoretically and experimentally derived  
8 relationships between velocity and external load. In low-pressure regions the amplitudes and  
9 frequencies of the reflected signals completely depend on the density of fractures and the load  
10 applied to them. And the earth material (its elastic moduli) significantly influences the amplitude  
11 parameters of the signals only at the loads close to the strength limit of discrete media.

12 What is needed then is a method for improving the ability to discover hydrocarbons in a  
13 subterranean formation and which makes use of available data, an in particular seismic data which  
14 is likely to be collected as part of a exploratory effort in any event.

## 15 16 **SUMMARY OF THE INVENTION**

17 The presented invention has been developed as a method for seismic data interpretation  
18 targeted at discovery of the areas of the accumulations of the fluids. We have discovered a  
19 relationship between reflection coefficient and general rock pressure, which is the basis of our  
20 invention. It is assumed that the real sedimentary sequence is a discrete medium subjected to  
21 inhomogeneous stresses created by two types of the forces, namely gravitational and tectonic forces.  
22 As a result of a sum influence of these two forces, the basin, as a discrete system, is found in  
23 continuous movement or in the condition of inhomogeneous stresses. In correspondence with this

1 point of view any stratigraphic sequence is found in different stress conditions in lateral direction,  
2 and consequently the amplitude and frequency parameters of reflected signals depend on the value  
3 of rock pressure acting on given element of a seismic reflector.

4 The first step of the developed interpretation method consists in tracking one or several  
5 target reflections along stacked time sections. A standard tracking procedure and standard 2D or 3D  
6 processing flows are used. The pressure gradients are found using picked travel times for tracked  
7 seismic horizons and by calculating parameters of Hillbert transformation (instantaneous  
8 amplitudes and phases) for each identified signal. The interpretation formula is directed to  
9 estimation of relative pressure changes under the assumption that the smoothed values of  
10 instantaneous amplitudes and derivatives of instantaneous phases (instantaneous frequency)  
11 correspond to general normal or gravitational pressure within all the study area, while all deviations  
12 from the average value represent relative estimates of anomalous pressures and correspond to local  
13 regions of decompression and compression.

14 The obtained map of relative pressure gradients is laid over the isochron map of a tracked  
15 horizon improved using the instantaneous phase picking. The principle of determining traveltimes  
16 more accurately consists in correction for signal frequency variation along the reflecting horizon in  
17 correspondence with the derived dependence of the frequency from pressure. The resulting map of  
18 relative pressure variation in combination with reflection time map represents the basis for  
19 identifying most probable locations of fluid accumulations. Localized region of anomalous  
20 unloading coincident with a closed or semi-closed time high is a physically valid area of  
21 hydrocarbon and water accumulation.

22 The information from the resulting map of relative pressure variation in combination with  
23 reflection time map can be further combined with classical seismic interpretation techniques to  
24 further enhance the prediction of the presence of fluids in a subterranean formation.

1        While the invention described herein is particularly useful for predicting the presence of  
2        fluid accumulations in a subterranean reservoir, the relationship between reflection coefficient and  
3        general rock pressure can also be used to predict rock pressure or pressure gradients within a  
4        subterranean formation. Such information can be useful in and of itself, for example, in the study  
5        and prediction of earthquakes.

6        The invention further includes a method for predicting the dynamic parameters of fluids in  
7        a subterranean reservoir. More specifically, the dynamic parameters of such fluids are  
8        determined by determining the relative estimate of the total ground pressure on the attributes of  
9        seismic signals related to a reflecting horizon, or any selected interval of the seismic section.  
10       This provides for a method for determining the location of the accumulation fluids in a  
11       subterranean formation. The method includes the steps of determining a first velocity vector  
12       " $V_x$ " for migration of fluid in a region of interest in the subterranean formation. The first  
13       velocity vector includes attributes of speed and direction of flow of fluid in a first direction in the  
14       region of interest. The method further includes determining a second velocity vector " $V_y$ " for  
15       migration of fluid in the region of interest. The second velocity vector includes attributes of  
16       speed and direction of flow of fluid in a second direction in the region of interest. The velocity  
17       vectors are then extrapolated to identify the fluid accumulation location. The first and second  
18       velocity vectors are primarily functions of supplementary pressure " $dP$ " in the region of interest,  
19       the permeability " $c$ " of the region of interest, and the viscosity " $u$ " of the fluid in the region of  
20       interest.

21       The supplementary pressure can be determined by identifying pressure gradients within the  
22       region, the region being characterized by a seismic image of a stacked time section representing  
23       horizons within the region. The permeability of the media within the region, and the viscosity of  
24       the fluid within the region, can either be determined mathematically or from geological data.

1        In addition to the methods disclosed and described herein, our invention further includes  
2        computer apparatus for implementing the methods.

3

4        **BRIEF DESCRIPTION OF THE DRAWINGS**

5        The file of this patent contains at least one drawing executed in color. Copies of this patent  
6        with color drawing(s) will be provided by the Patent and Trademark Office upon request and  
7        payment of the necessary fee.

8        FIG.1 illustrates the principle of relative pressure calculations for a given seismic horizon  
9        on a stacked time section.

10       FIG.2 shows a flow chart of the method for calculating anomalous pressure estimates and  
11       corrections for reflection traveltimes distortions using a set of stacked seismic sections processed  
12       with the aid of 3D techniques.

13       FIG.3 is an example of anomalous pressure map for producing sandy-argillaceous Jurassic  
14       formation.

15       FIG.4a shows an isochron map constructed using a standard technique of reflection horizon  
16       tracking.

17       FIG. 4b shows a map of traveltimes corrections for variation in signal frequencies along the  
18       reflection horizon.

19       FIG. 5 shows the final anomalous pressure map laid over isochron map and exploratory  
20       well locations.

21       FIG. 6 depicts a three-layer model of the medium of a subterranean formation having  
22       discrete structure.

23       FIG. 7 depicts two qualitative graphs of the parameters of fluid flow in a thin discrete  
24       layer: graph "a" depicts pressure gradients in the presence of two-axis anisotropy; and graph "b"  
E:\Files\Trans Seismic\TR01-004-PA1.doc, 12/01/99

1 depicts pressure gradients in the presence of triaxial anisotropy.

2 FIG. 8 depicts the method for determining the fluid-dynamic parameters on a seismic  
3 section.

4

5 **DETAILED DESCRIPTION OF THE INVENTION**

6 Taking into account the information known which is discussed in the Background section  
7 above, we concluded that each layer or stratigraphic unit of a sedimentary basin is subjected to  
8 variable load along its extent. In one location the layer will have a high load (for example, equal to  
9 the normal lithostatic or gravitational pressure), while in the other location the load can be  
10 significantly lower, thus leading to the presence of a decompressed zone where reduction of general  
11 rock pressure is associated with fracture opening. Our invention makes use of this observation  
12 since one may predict what will happen to the fluid occupying the pore space of a continuous rock  
13 as well as interconnected system of fractures. That is, the fluid, particularly its light fractions, will  
14 migrate from the regions of relatively high pressure toward the decompressed zone, and if the  
15 closure conditions exist, accumulation and preservation of the accumulation of any type of fluid  
16 will take place. It should be noted that the presence of simple anticlinal structures is not necessary,  
17 and an accumulation can be formed in absolutely non-traditional conditions. The main factors in  
18 this case are the degree of discreteness of a given layer (the spatial density of fractures) and relative  
19 change in the general pressure.

20 Hence, we determined that if one knows the relative distribution of the general stress within  
21 all the sedimentary sequence or within its producing interval, it is possible to establish an objective  
22 criterion for discovering subsurface fluids' accumulations independently from all known structural  
23 and lithological conditions favorable for such accumulation. Seismic data is the primary source of  
24 information for making the stress condition estimate. At the same time all existing methods and

1 techniques for seismic data interpretation are based on classical solutions to a wave equation for  
2 continuous and static media. In these solutions it is common to substitute stresses in initial wave  
3 equation by strains using the Hooke's law, i.e. using the elastic moduli. Therefore, the acoustic  
4 impedances or parameters derived from them are in practice the informative parameters for seismic  
5 data interpretation. But if the discrete dynamic model is used, the wave equation solution should be  
6 obtained for prestressed media, and the components of stress condition of real media are the target  
7 parameters. These parameters are of principal importance for exploring and discovering new oil and  
8 gas pools and water reserves as well as for planning their development.

9 Immediately following is a description containing the solution to a classical wave equation  
10 for a simple case of wave incidence on the interface between two half-spaces one of which is in  
11 prestress condition. We will now show our derivation of an expression for normal-incidence  
12 reflection coefficient for an elastic wave:

---

$$A_R = \frac{Z - Z^* + \Delta Z^*/\omega}{Z + Z^* + \Delta Z^*/\omega} \quad (3)$$

13 where  $A_R$  is reflection coefficient,  $Z$  and  $Z^*$  are acoustic impedances for unstressed half-space  
14 and prestressed half-space correspondingly, and  $\omega$  is circular frequency,

15  $\Delta Z^* = PZ^*\omega/\mu^*$  (4)

16 where  $P$  is a value proportional to non-hydrostatic pressure in the stressed half-space, and  $\mu^*$  is  
17 shear modulus in the stressed medium.

18  
19  
20 **Reflection and refraction coefficients for plane elastic waves propagating in a prestressed**  
21 **medium**

22 **1. Motion equations**

1 The main law of dynamics  $\mathbf{F}^{\rightarrow} = \mathbf{m} \mathbf{a}^{\rightarrow}$  has the following form for a continuous elastic

2 medium:

3

4

5

6

7

8

$$\rho \frac{\partial^2 \mathbf{u}_i}{\partial t^2} = \frac{\partial \mathbf{T}_{ij}}{\partial x_j} \quad (a)$$

9 where stress tensor divergence in the right part of the formula is equal to the force acting on the  
10 unit volume of an elastic body subjected to internal dynamic stresses.

11 The generalized Hooke's law can be written as follows:

12

13

14

15

16

17

18

19

20

21

22

23

$$\mathbf{T}_{ij} = c_{ijkl} \mathbf{S}_{kl} = c_{ijkl} \frac{\partial \mathbf{u}_l}{\partial x_k} \quad (b)$$

24 Here  $c_{ijkl}$  is the tensor of elastic moduli. Substitution of the formula (b) into the equation (a)  
25 results in

26

27

28

29

30

31

32

$$\rho \frac{\partial^2 \mathbf{u}_i}{\partial t^2} = c_{ijkl} \frac{\partial^2 \mathbf{u}_l}{\partial x_j \partial x_k} \quad (c)$$

33 For an isotropic solid body

34

35

36

37

38

39

40

41

42

43

44

45

46

$$c_{ijkl} = \lambda \delta_{ij} \delta_{kl} + \mu (\delta_{ik} \delta_{jl} + \delta_{il} \delta_{jk}) \quad (d)$$

47 We then assume that an elastic medium is found under the condition of static prestress,

48 caused by external forces, defectiveness of the medium, and other reasons. We further assume  
49 that prestresses are distributed in the medium continuously. In this case elastic wave propagation  
50 in a prestressed medium can be described as superposition of small dynamic strains to, in the  
51 general case, finite static strains. The linearized theory of elastic wave propagation in a

1 prestressed medium is correct under this assumption, and consequently elastic waves can be  
2 described by equation (3) where the tensor of elastic moduli is given by

3  $c_{ijkl}^+ = c_{ijkl}^* + \sigma_{ij}^0 \delta_{ik}$  (e)

4 - where  $c_{ijkl}^*$  are effective elastic moduli describing response of a prestressed elastic medium  
5 to small dynamic loads, and  $\sigma_{ij}^0$  is prestress tensor. By this means we have derived linearized  
6 motion equations for a prestressed elastic continuous medium in the form

7

8  $\rho \frac{\partial^2 u_i}{\partial t^2} = c_{ijkl}^+ \frac{\partial^2 u_i}{\partial x_j \partial x_k}$  (f)

9

10

11

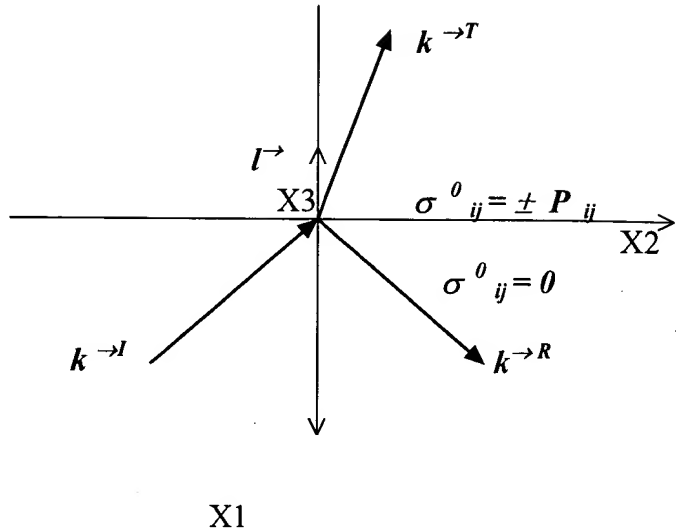
12

## 13 2. Problem formulation.

14 If one considers two elastic half-spaces having a tight planar contact, the elastic moduli  
15  $c_{ijkl}$  of the lower half-space which is not subjected to prestresses differs from the elastic  
16 moduli of the upper half-space because of different composing materials. Besides, material of the  
17 upper half-space is prestressed and described by the prestress tensor  
18  $\sigma_{ij}^0$ . In this way the elastic moduli of the upper half-space have the form (e). We then consider  
19 a plane wave incident on the interface from the lower half-space. Our problem then has the  
20 following formulation: it is required to determine propagation direction, polarization, and  
21 reflection and refraction amplitudes for known propagation direction, polarization, and amplitude  
22 of the incident wave and specified elastic moduli of both half-spaces.

23

24



Boundary conditions for a tight contact require strain and stress continuity to be met at any moment of time and at any point of the contact surface specified in this case by the equation  $l^r \cdot x^r = 0$ , where  $l^r$  - is the vector normal to the contact surface, and  $x^r$  - is coordinate in the contact plane  $X_2OX_3$ . The conditions of strain and stress continuity can be written as follows

$$u_i^I + \sum_R u_i^R = \sum_T u_i^T \quad (g)$$

$$T_i^I + \sum_R T_i^R = \sum_T T_i^T \quad (h)$$

Here we use the following indices: **I**- for incident waves, **R** -for reflected waves, and **T**- for refracted waves.

We then consider the following type of monochromatic waves

$$u_i = {}^0 u_i e^{i(\omega t - k \cdot x)} \quad (i)$$

where  ${}^0 u_i = u_0 p_i$ ,  $u_0$  - is wave amplitude,  $p_i$  - is polarization vector.

The strain continuity condition (g) has the following form for the wave (i)

$$\begin{aligned} & \sum_i^R \mathbf{u}_i^R \exp \{i(\omega^R t - \mathbf{k}^R \cdot \mathbf{x})\} + \sum_i^T \mathbf{u}_i^T \exp \{i(\omega^T t - \mathbf{k}^T \cdot \mathbf{x})\} = \\ & = \sum_i^T \mathbf{u}_i^T \exp \{i(\omega^T t - \mathbf{k}^T \cdot \mathbf{x})\} \end{aligned} \quad (j)$$

It follows from the formula (j) that at any moment of time

$$\omega^I = \omega^R = \omega^T \quad (k)$$

and at any point of the contact surface

$$\mathbf{k}^I \cdot \mathbf{x} = \mathbf{k}^R \cdot \mathbf{x} = \mathbf{k}^T \cdot \mathbf{x} \quad (l)$$

We thus derive the following formulae from the equations (l)

$$(\mathbf{k}^R - \mathbf{k}^I) \cdot \mathbf{x} = 0, \quad (\mathbf{k}^T - \mathbf{k}^I) \cdot \mathbf{x} = 0$$

By comparison with the contact surface equation  $\mathbf{l} \cdot \mathbf{x} = 0$ , one will see that that the vectors

$(\mathbf{k}^R - \mathbf{k}^I)$  and  $(\mathbf{k}^T - \mathbf{k}^I)$  are perpendicular to the contact surface.

All of the wavenumber vectors lie in the incidence plane specified by the normal  $\mathbf{l}$  and

wavenumber vector  $\mathbf{k}^I$ . Projections of all wavenumber vectors to the contact plane are equal to

each other. We thus get

$$\mathbf{k}^R \sin \theta^R = \mathbf{k}^T \sin \theta^T = \mathbf{k}^I \sin \theta^I$$

Since the frequency content of the reflection wavelets is the same, the directions of wave

propagation are determined from the following relations:

$$\sin \theta^R / V(\theta^R) = \sin \theta^T / V(\theta^T) = \sin \theta^I / V(\theta^I)$$

Now we derive simplified boundary conditions for strains from the formula (j)

$$\sum_i^R \mathbf{u}_i^R + \sum_i^T \mathbf{u}_i^T = \sum_i^T \mathbf{u}_i^T \quad (m)$$

Substitution of the formula (9) into the Hooke's law (b) gives the following

$$T_{ijkl} = -i c_{ijkl} \sum_k \mathbf{u}_k \exp \{i(\omega t - \mathbf{k} \cdot \mathbf{x})\}$$

1  
2 The boundary conditions for stresses (h) now have the form  
3

4 
$$c_{ijkI} [k_I^I \overset{0}{u}_k^I + \sum_R k_R^R \overset{0}{u}_k^R] = c^+_{ijkI} \sum_R k_I^T \overset{0}{u}_k^T \quad (n)$$
  
5

6 Here the elastic moduli of stressed medium  $c^+_{ijkI}$  are determined from the formula (e).

7 To simplify further our conclusions we assume that internal stresses determined by the  
8 initial stress tensor  $\sigma_{ij}^0$  do not violate the medium isotropy, i.e. the tensor  $\sigma_{ij}^0$  is isotropic:  
9  $\sigma_{ij}^0 = \pm P \delta_{ij}$ . Here  $P$  is the tensor diagonal or a value proportional to the pressure (sign +  
10 corresponds to relief, and sign - corresponds to compression) in a stressed medium.

11

### 12 3. Particular case of a plane shear wave with horizontal polarization (SH-wave).

13 For further conclusions we specify propagation direction and polarization of the incident  
14 wave. To simplify computations I select SH-wave as an incident wave. With this selection only  
15 two waves will appear the contact surface, i.e. reflected wave and refracted wave with the same  
16 polarization as that of the incident wave. So we have

17 
$$\overset{0}{u}_i = \overset{0}{u} p_i = \overset{0}{u} \delta_{i3}$$

18 for each wave. Substitution of this expression into (m) results in

19 
$$\overset{0}{u}^I + \overset{0}{u}^R = \overset{0}{u}^T \quad (o)$$
  
20

21 Condition  $I_j = -\delta_{j1}$  is satisfied for the normal  $I^j$ , and  $\overset{0}{u}_k = \overset{0}{u} \delta_{k3}$

22 Now instead of (n) we derive

23 
$$c_{ij3I} [k_I^I \overset{0}{u}^I + k_R^R \overset{0}{u}^R] = c^+_{ij3I} k_I^T \overset{0}{u}^T \quad (p)$$

24 Since wavenumber vectors lie in the plane defined by the normal  $I^j$  and the  
25 wavenumber vector  $k^R$  of the incident wave, they have only two components (in the axes  $X_1$   
26 and  $X_2$ ). By performing summation with respect to the index  $I$  we convert the expression (p) to

$$c_{i131} [k^I_1 {}^0\mathbf{u}^I + k^R_1 {}^0\mathbf{u}^R] + c_{i132} [k^I_2 {}^0\mathbf{u}^I + k^R_2 {}^0\mathbf{u}^R] = \\ = c^+_{i131} k^T_1 {}^0\mathbf{u}^T + c^+_{i132} k^T_2 {}^0\mathbf{u}^T \quad (q)$$

Taking into account our assumption about initial stress tensor isotropy ( $\sigma^0_{ij} = \pm P \delta_{ij}$ ), we derive equation (4) into the following expression for the elastic moduli contained in equation (q)

$$c_{i131} = \lambda \delta_{i1} \delta_{31} + \mu (\delta_{i3} \delta_{11} + \delta_{i1} \delta_{13})$$

$$c_{i132} = \lambda \delta_{i2} \delta_{32} + \mu (\delta_{i3} \delta_{12} + \delta_{i2} \delta_{13})$$

It can thus be seen from the latter that only the elastic modulus is not equal to zero for an

isotropic medium. So instead of expression (q) we derive

$$c_{3131} [k^I_1 {}^0\mathbf{u}^I + k^R_1 {}^0\mathbf{u}^R] = c^+_{3131} k^T_1 {}^0\mathbf{u}^T \quad (r)$$

We now have a system of equations

$$\left\{ \begin{array}{l} {}^0\mathbf{u}^I + {}^0\mathbf{u}^R = {}^0\mathbf{u}^T \\ c_{3131} [k^I_1 {}^0\mathbf{u}^I + k^R_1 {}^0\mathbf{u}^R] = c^+_{3131} k^T_1 {}^0\mathbf{u}^T \end{array} \right. \quad (s)$$

We next introduce the reflection and refraction coefficients by definition

$$A_R = \frac{{}^0\mathbf{u}^R}{{}^0\mathbf{u}^I}$$

$$A_T = \frac{{}^0\mathbf{u}^T}{{}^0\mathbf{u}^I}$$

Then we have the following solution to the equation system (s)

$$1 \quad A_T = A_R + I \\ 2 \quad (t)$$

$$3 \quad \begin{aligned} 4 \quad A_R = & \frac{c^+_{3131} k^T_1 - c_{3131} k^I_1}{c_{3131} k^R_1 - c^+_{3131} k^T_1} \\ 5 \\ 6 \\ 7 \end{aligned} \quad (u)$$

8 Taking into account that  $c_{3131} = \mu$  in an isotropic medium, and using the formula (e) and  
 9  $\sigma_{ij}^\theta = \pm P \delta_{ij}$  we derive from (u)

$$10 \quad \begin{aligned} 11 \quad A_R = A_R(P) = & \frac{\mu^* k^T_1 - \mu k^I_1 \pm P k^T_1}{\mu k^R_1 - \mu^* k^T_1 \pm P k^T_1} \\ 12 \\ 13 \\ 14 \end{aligned} \quad (v)$$

15 By substituting  $k^R_1 = -k^I_1 = k^I \cos \theta^I$ ,  $k^T_1 = -k^T \cos \theta^T$  we obtain

$$16 \quad \begin{aligned} 17 \quad A_R = & \frac{\mu k^I \cos \theta^I - (\mu^* \pm P) k^T \cos \theta^T}{\mu k^I \cos \theta^I + (\mu^* \pm P) k^T \cos \theta^T} \\ 18 \\ 19 \\ 20 \\ 21 \\ 22 \end{aligned} \quad (w)$$

23 After introduction of acoustic impedances of shear waves  $Z_3 = \rho V_3$ ,  $Z^*_3 = \rho^* V^*_3$ , we obtain

$$10 \quad 1 \quad k' \mu = \frac{\omega \mu}{V_3} = \frac{\omega \rho (V_3)^2}{V_3} = \omega Z_3$$

$$5 \quad k^T \mu^* = \omega Z^* \quad 3$$

6 Introducing notation

$$7 \quad \Delta Z^* = P k^T$$

8 we finally obtain:

$$9 \quad 10 \quad 11 \quad 12 \quad 13 \quad A_R = \frac{Z_3 \cos \theta^I - (Z_3^* \pm \Delta Z^*/\omega) \cos \theta^T}{Z_3 \cos \theta^I + (Z_3^* \pm \Delta Z^*/\omega) \cos \theta^T} \quad (x)$$

14  
15 The formulae (u)-(x) show that the reflection coefficient and consequently the refraction  
16 coefficient depend on the stress condition of the other half-space. Similar results can be obtained  
17 for compressional waves and for the case where both half-spaces are prestressed. Formulae for  
18 reflection coefficients for the said variants differ from the formula (x) only by constants.

### 20 *Inventive results of the derivation: The Method and its Application*

21 The expression (3) is different from the classical one by an additional member ( $\Delta Z^*/\omega$ )

22 which depends on the difference between stress conditions of the upper and lower half-spaces.

23 Taking into account the fact that in a discrete medium the elastic moduli have little effect on the

24 changes in stress condition, the expression (3) can be rewritten in the form:

$$25 \quad 26 \quad 27 \quad 28 \quad A_R = \frac{\Delta Z^*/\omega}{2Z + \Delta Z^*/\omega} \quad (5)$$

29 If we assume that the elastic moduli do not vary along given reflecting boundary, while pressure  $P$   
30 varies, and the reflection coefficients in two points  $L$  and  $M$  of the reflecting boundary are given by

$$\frac{A^L_R}{A^M_R} = \frac{\Delta Z^*_L \omega_M (2Z + \Delta Z^*_M / \omega_M)}{\Delta Z^*_M \omega_L (2Z + \Delta Z^*_L / \omega_L)} \quad (6)$$

T0190  
Taking into account the expression (4) the formula (6) can be rewritten in the following form with  
accuracy up to a constant:

$$\frac{dP}{P_M} \approx \frac{(A^L_R)^a (\omega_M)^2}{(A^M_R)^a (\omega_L)^2}; \quad (7)$$

Where:  $a = 2$  for the media with high moduli (carbonate basins), and  $a = 1$  for the media with  
low moduli (terrogenous basins).

By this means the value  $dP$  is a relative estimate of pressure changeability along a seismic  
reflector. For a stacked time section the amplitude of signal is proportional to the reflection  
coefficient for given reflecting boundary, and we modify expression (7) to contain analytical signal  
parameters:

$$dP^L(t_i) = \frac{(a^L(t_i))^a (dF^L/dt)^2}{(a^0(t_i))^a (dF^L/dt)^2} \quad (8)$$

where  $a(t) = (u^2(t) + v^2(t))^{1/2}$ ,  $F(t) = \arctg(v(t)/u(t))$  is Hillbert transformation, and  $a(t)$  and  $dF/dt$   
are instantaneous amplitudes and frequencies correspondingly. Instead of substitution of the  
parameters at the point  $M$  we use the following idea: amplitude parameters  $a^0(ti)$  and  $dF^0/dt$   
smoothed over the whole horizon represent a model of normal lithostatic pressure, or which is the  
same, "automatically" account for unknown elastic moduli of the medium.

We then apply expression (8) in the method for estimating pressure gradient on a stacked time  
section under the following assumptions:

1 -  $a^0(ti)$  and  $dF^0/dt$  are determined as average values of the instantaneous amplitudes and  
2 frequencies for the whole reflecting horizon or some its part taking into account little variability  
3 and influence of the elastic moduli of the rocks within a local part of the basin comparatively to  
4 the scale of sedimentary process,

5 - if  $dP(ti)$  is greater than unity, this indicates a reduction of the general pressure at a given point  
6 with respect to the average (normal or gravitational) pressure, which indicates a region of  
7 unloading,

8 - if  $dP(ti)$  is less than unity, this indicates an increase of the general pressure up to the normal  
9 (average) value or, which is less probable for discrete media, up to a value exceeding the  
10 normal pressure.

11 FIG.1 illustrates the principle of calculating parameters used in the formula (8). Time section  
12 for the seismic line 10 is an example of standard 3D processing in the area of detailed exploration  
13 for oil. Graph 10a shows geometry of the tracked reflecting horizon "C" coincident with the top of  
14 producing stratigraphic sequence in the terrigenous basin (sandy-argillaceous Jurassic formations).  
15 The fragments 16 and 18 show intervals of two traces 2 ( $Tm$ ) and 5 ( $Tn$ ) corresponding to said  
16 horizon at the points 12 and 14. Also shown here are the results of Hillbert transformation of these  
17 traces: 4 and 7 - instantaneous amplitude ( $A$ ), and 3 and 6 - instantaneous phase ( $F$ ). The points  $t^m_c$   
18 and  $t^n_c$  indicate position of the tracked horizon "C" after a standard picking procedure via the  
19 extrema of reflected wavelet.

20 To obtain stable values of parameters contained in the formula (8) the following steps are  
21 performed:

22 - find a singular point on the phase curve  $F$  closest to the point  $t^m_c$  (the curve F crosses zero  
23 at the point  $t^m_{CR}$ ),

1 - find the previous singular point on the phase curve  $F$  closest to the point  $t^m CR$  (the curve  
 2  $F$  crosses value of 180 degrees at the point  $t^{m1} CR$  ),  
 3 - find the following singular point on the phase curve  $F$  closest to the point  $t^m CR$  (the  
 4 curve  $F$  crosses value of 180 degrees at the point  $t^{m2} CR / dt$ ),  
 5 - in the time window specified as described above the normalized values of instantaneous  
 6 amplitude and instantaneous frequency are given by

7

8  $t^{m2} CR / dt$

---

9

10

11

12  $A^m c = \frac{\sum a_i}{t^{m1} CR / dt}$

13  $(t^{m2} CR - t^{m1} CR) / dt$

14

15

16

17

18

19

20  $f^m c = \frac{t^{m2} CR / dt}{\sum (F_i - F_{i+1}) / dt}$

21  $t^{m1} CR / dt$

22

23

24

(9)

25

26

27

28

29

30  $A^m c$  and  $f^m c$  are calculated for all points  $t_c$  of the horizon "C" for a  
 31 given section. As a result we obtain two sets of the normalized values of instantaneous amplitudes  
 32 and frequencies and after that calculate average values of  $A^0 c$  and  $f^0 c$  using the following formulae:

---

33

34

35

36

37

38

39

40

41

42

43

44

45

46

47

48

49

50

51

52

53

54

55

56

57

58

59

60

61

62

63

64

65

66

67

68

69

70

71

72

73

74

75

76

77

78

79

80

81

82

83

84

85

86

87

88

89

90

91

92

93

94

95

96

97

98

99

100

101

102

103

104

105

106

107

108

109

110

111

112

113

114

115

116

117

118

119

120

121

122

123

124

125

126

127

128

129

130

131

132

133

134

135

136

137

138

139

140

141

142

143

144

145

146

147

148

149

150

151

152

153

154

155

156

157

158

159

160

161

162

163

164

165

166

167

168

169

170

171

172

173

174

175

176

177

178

179

180

181

182

183

184

185

186

187

188

189

190

191

192

193

194

195

196

197

198

199

200

201

202

203

204

205

206

207

208

209

210

211

212

213

214

215

216

217

218

219

220

221

222

223

224

225

226

227

228

229

230

231

232

233

234

235

236

237

238

239

240

241

242

243

244

245

246

247

248

249

250

251

252

253

254

255

256

257

258

259

260

261

262

263

264

265

266

267

268

269

270

271

272

273

274

275

276

277

278

279

280

281

282

283

284

285

286

287

288

289

290

291

292

293

294

295

296

297

298

299

300

301

302

303

304

305

306

307

308

309

310

311

312

313

314

315

316

317

318

319

320

321

322

323

324

325

326

327

328

329

330

331

332

333

334

335

336

337

338

339

340

341

342

343

344

345

346

347

348

349

350

351

352

353

354

355

356

357

358

359

360

361

362

363

364

365

366

367

368

369

370

371

372

373

374

375

376

377

378

379

380

381

382

383

384

385

386

387

388

389

390

391

392

393

394

395

396

397

398

399

400

401

402

403

404

405

406

407

408

409

410

411

412

413

414

415

416

417

418

419

420

421

422

423

424

425

426

427

428

429

430

431

432

433

434

435

436

437

438

439

440

441

442

443

444

445

446

447

448

449

450

451

452

453

454

455

456

457

458

459

460

461

462

463

464

465

466

467

468

469

470

471

472

473

474

475

476

477

478

479

480

481

482

483

484

485

486

487

488

489

490

491

492

493

494

495

496

497

498

499

500

501

502

503

504

505

506

507

508

509

510

511

512

513

514

515

516

517

518

519

520

521

522

523

524

525

526

527

528

529

530

531

532

533

534

535

536

537

538

539

540

541

542

543

544

545

546

547

548

549

550

551

552

553

554

555

556

557

558

559

560

561

562

563

564

565

566

567

568

569

570

571

572

573

574

575

576

577

578

579

580

581

582

583

584

585

586

587

588

589

590

591

592

593

594

595

596

597

598

599

600

601

602

603

604

605

606

607

608

609

610

611

612

613

614

615

616

617

618

619

620

621

622

623

624

625

626

627

628

629

630

631

632

633

634

635

636

637

638

639

640

641

642

643

644

645

646

647

648

649

650

651

652

653

654

655

656

657

658

659

660

661

662

663

664

665

666

667

668

669

670

671

672

673

674

675

676

677

678

679

680

681

682

683

684

685

686

687

688

689

690

691

692

693

694

695

696

697

698

699

700

701

702

703

704

705

706

707

708

709

710

711

712

713

714

715

716

717

718

719

720

721

722

723

724

725

726

727

728

729

730

731

732

733

734

735

736

737

738

739

740

741

742

743

744

745

746

747

748

749

750

751

752

753

754

755

756

757

758

759

760

761

762

763

764

765

766

767

768

769

770

771

772

773

774

775

776

777

778

779

780

781

782

783

784

785

786

787

788

789

790

791

792

793

794

795

796

797

798

799

800

801

802

803

804

805

806

807

808

809

810

811

812

813

814

815

816

817

818

819

820

821

822

823

824

825

826

827

828

829

830

831

832

833

834

835

836

837

838

839

840

841

842

843

844

845

846

847

848

849

850

851

852

853

854

855

856

857

858

859

860

861

862

863

864

865

866

867

868

869

870

871

872

873

874

875

876

877

878

879

880

881

882

883

884

885

886

887

888

889

890

891

892

893

894

895

896

897

898

899

900

901

902

903

904

905

906

907

908

909

910

911

912

913

914

915

916

917

918

919

920

921

922

923

924

925

926

927

928

929

930

931

932

933

934

935

936

937

938

939

940

941

942

943

944

945

946

947

948

949

950

951

952

953

954

955

956

957

958

959

960

961

962

963

964

965

966

967

968

969

970

971

972

973

974

975

976

977

978

979

980

981

982

983

984

985

986

987

988

989

990

991

992

993

994

995

996

997

998

999

1000

1 Finally, use the formula (8) to determine pressure gradients (i.e. relative changeability of pressure)  
2 in each point of given horizon "C":

3  $dP^i (t^i c) = (A^i c / A^0 c)^a (f^0 c / f^i c)^2$  (12)

4 Assumedly the exponent "a" for a terrigenous basin is equal to unity. Finally we determine  
5 new values of  $t^i c$  corrected for variation in the frequency spectrum of reflected wavelets along the  
6 horizon "C". As is evident from the FIG.1, the differences  
7  $\Delta t m = t^{m1} c_R - t^{m0} c_R$  and  $\Delta t n = t^{n1} c_R - t^{n0} c_R$  for two traces 12 (**m**) and 14 (**n**) are not equal  
8 to each other because of difference in frequency content of the same reflection in two distant points  
9 of the tracked horizon. Consequently, all the values  $t^i c$  should be corrected as follows:

10  $t^{i new} c = t^i c - 2(1/f^i c - 1/f^0 c)$  (13)

11 It should be appreciated that the map of pressure gradients which is generated using Eqn.  
12, an example of which is shown in Fig. 3, can be of value in and of itself for identifying regions  
13 of differential rock pressure. Such can be used for example in the study of earthquakes, including  
14 predicting areas of likely seismic activity.

15 FIG.2 represents the complete chart of the proposed seismic data interpretation method  
16 targeted at determining relative pressure estimates and locating oil and gas fields. Preferably the  
17 input data for the interpretation method are stacked time sections obtained as a result of standard  
18 2D or 3D processing. In a first embodiment the interpretation scheme is applied to the results of 3D  
19 processing. The input data are, for example, the set of stacked time sections (gathered in in-line or  
20 on-line direction) marked in the FIG.2 by blocks 20, 40 and 42. The process, preferably, starts from  
21 the section 22. At first, a selected horizon is picked in manual or automatic mode using a generally  
22 accepted principle of tracking via the extrema of wavelets belonging to this horizon. The picked  
23 traveltimes  $t^i c$  are, preferably, saved in the matrix 34 and transmitted to the following step 24

1 where the Hillbert transformation is preferably performed.

2 At the step 26, the picked traveltimes  $t^i c$  are advantageously used to calculate normalized  
3 values of instantaneous amplitudes and frequencies  $A^i c$  and  $f^i c$  using the formulae (9) and (10).  
4 Then, at the step 28, we advantageously determine the average values  $A^0 c$  and  $f^0 c$  for obtained data  
5 sets. At the step 30, desired values of relative pressure changeability  $dP^i$  are advantageously found  
6 and the obtained data set is preferably saved in the matrix 36. At the step 32 we advantageously  
7 determine corrections for signal frequency variability and correct the values  $t^{i \text{ new}} c$  preferably  
8 using the formula (13). The corrected traveltime values are preferably saved in the matrix 38.

9 Then all the before mentioned steps are preferably applied to the section 40 and so on until  
10 the steps have been applied to all sections. When the last section (42) has been processed, we will  
11 have filled matrices 34, 36, and 38, which can be used for generating the following maps: initial  
12 isochron map, pressure gradient map, and corrected isochron map. These maps are the basis for  
13 identifying the most probable locations of oil, gas, water and other fluid accumulations.

14 FIG.3 shows a relative pressure changeability map (44) for the producing horizon “ C “.  
15 The map has been created using the described scheme for an oil field in the terrigenous basin. The  
16 regions of anomalously low relative pressure values, of which 80, 82 and 84 are representative,  
17 have been shaded red and represent a hydrocarbon indicator for fractured reservoirs in sandy-  
18 argillaceous Jurassic formations. The obtained result is then compared with the reflector geometry  
19 which is shown in FIGS. 4a and 4b.

20 FIG. 4a shows an isochron map for given horizon (fragment 46) and FIG. 4b shows a map  
21 of traveltime corrections  $dt c$  (fragment 48). Several positive anomalies of traveltime corrections  
22 can be seen in FIG. 4b. If we apply the traveltime corrections, new anticlinal structures (namely 50,  
23 52, and 54) not previously detected on the results of standard horizon picking appear on the  
24 traveltime map. Vertical closures of the newly delineated structures are of 20-30 m, the value of

1 great importance for the region of low-relief oil-bearing structures.

2 FIG.5 shows final interpretation results: the relative pressure changes map (FIG.3) has been  
3 laid over corrected isochron map shown in the FIG.4a. The isochrons have been drawn as contours  
4 while the value of the relative pressure changeability estimates have been indicated using a color  
5 palette. The red shading (e.g., 58 and 68) corresponds to anomalously low values of changeability,  
6 while blue shading (e.g., 90) corresponds to normal lithostatic pressures.

7 Analysis of the map of FIG. 5 brings us to the following conclusions:

8 - low-pressure regions (58, 60, 62, 64, 66, 68 and 70) are localized;  
9 - these regions coincide with highs on the isochron map of FIG. 4a;  
10 - the regions 58,60, and 62 coincide with previously discovered oil fields which verifies the high  
11 quality and fidelity of our method for predicting the presence of fluid;  
12 - the regions 64, 66, 68 and 70 should be therefore recommended for exploratory drilling.

13 At the final step, the depth map for producing the horizon is advantageously constructed by  
14 implementing a standard time-to-depth conversion technique to the corrected isochron map (48).  
15 This map together with pressure estimates and recommended exploratory drilling locations can be  
16 used at the prospect evaluation stage as well as at the field development planning stage, because the  
17 estimates of relative pressures in the reservoir can have the key role while selecting methods and  
18 technologies of oil production, like in this particular case.

19 It is to be appreciated that the method described can, as suggested in the above paragraph,  
20 further include using classical, and future, discovered, seismic interpretation techniques in  
21 conjunction with the resulting pressure-isochron map. For example, classical seismic interpretation  
22 techniques are useful for identifying faults and traps which can cause fluids to accumulate in a  
23 subterranean reservoir. When an area of interest identified by the pressure-isochron map  
24 corresponds with the presence of a fluid trap, the likelihood that fluids are present in the identified

1 area is increased.

2 The described methods are preferably performed using a computer. Thus, the invention  
3 further includes a computer configured to carry out the disclosed methods. The computer is  
4 configured to read a computer readable medium or computer memory which contains computer-  
5 executable steps for performing the steps of the method shown and described in the chart of Fig. 2.  
6 Generally, sets of computer-executable instructions for performing seismic data processing and  
7 generating resulting maps or seismic sections for interpretation are common in the industry, and in  
8 fact constitute the typical manner by which seismic methods are carried out. Examples of computer  
9 readable medium include a hard drive, a tape drive, a diskette, and ROM (read only memory)  
10 devices, such as a compact disk. Examples of computer readable memory include a hard drive and  
11 RAM (random access memory). As a result of performing the computer-executable steps on an  
12 appropriate input data set, the computer produces a product data set. The product data set can be  
13 outputted in the form of charts or graphs which are indicative of relative pressure changeability  $dP^i$   
14 of a subterranean region, pressure gradients in the region, corrected traveltimes values  $t^{i \ new}$   $c$  of the  
15 region, or any of the following maps: an initial isochron map, a pressure gradient map, a corrected  
16 isochron map, or an overlay of the relative pressure changeability map and the corrected isochron  
17 map. As indicated earlier, these maps are the basis for identifying the most probable locations of  
18 oil, gas, water and other fluid accumulations.

19

20 **Method For Predicting The Dynamic Parameters Of Fluids In A Subterranean Reservoir**

21 It is known that oil and gas pools in a sedimentary basin are formed as a corollary of three  
22 main interconnected processes: generation, migration and accumulation. Existing technologies  
23 for studying reservoirs using geological and geophysical data to identify such oil and gas pools  
24 are targeted at detection of probable locations of fluid accumulation, known as "traps". Current

1 methods for trap detection do not necessary lead to success in identifying such traps, however,  
2 due to many technical, geological, and other factors. However, we have developed a different  
3 approach to identifying traps having the probability of fluid presence, comprising estimation of  
4 the parameters of fluid flow or migration flow. Specifically, by determining the main parameters  
5 of the migration flow, for example its speed and direction, then the anomalous values of these  
6 parameters can correspond to the location of a trap. This method allows for the detection of traps  
7 where prior detection efforts, using attributes such as structural images of the reflecting interfaces  
8 and acoustic impedance, would be unsuccessful. The method of the present invention allows for  
9 parameters of migration flow to be determined by determining the relative estimate of the total  
10 ground pressure on the attributes of selected seismic signals.

11 The invention thus further includes a method for determining the relative estimate of the  
12 total ground pressure  $dP$  on the attributes of the seismic signals related to a reflecting horizon, or  
13 any selected interval of the seismic section. In terms of geodynamics in a subterranean reservoir  
14 or basin system in question, we start by assuming that:

$$P(T) = P_g \pm dP(T) \quad (\text{Eqn. 14})$$

16 where:

17  $P(T)$  - is the total ground pressure at given depth and at given point in geological time;

18  $P_g$  - is the normal lithostatic pressure; and

19  $dP(T)$  - is the supplementary pressure caused by the basin motion at the same point in  
20 geological time.

21 Thus, by obtaining a relative estimate of the total ground pressure  $dP(T)$  for a reflecting  
22 horizon using the seismic data, we then have a method for calculating the parameters

23

1 →  
 2  $V(T)$ ,  $c$  and  $\mu$  on the basis of Equation (14) using certain assumptions about the model of the  
 3 fracture-porous volume of the medium in the studied interval of the subsurface and the ratio of  
 4 solid and liquid components of the total supplementary pressure  $dP(T)$ .  
 5

6 Recognizing the generally accepted scheme of destruction of a sedimentary basin, we can  
7 assume that the response of a discrete medium to the basement movements caused by current  
8 geodynamics of the lithosphere is formed in a slowed rate in the form of a viscous flow.  
9 Consequently, we can make a principal assumption about the property of continuity of solid and  
10 liquid components of the total pressure and further consider  $dP(T)$  as over-hydrostatic pressure  
11 which we will notify as  $P_d$ .

12 This approach allows us to solve constructively the problem of fluid migration as applied  
 13 to the geodynamic history of a basin's development. In this case the speed and direction of a fluid  
 14 flow  $\vec{V}$  are expressed in the following form in correspondence with Equation (14):

$$\vec{V}(T) = -(c/\mu) \nabla dP(T) \quad (\text{Eqn. 15})$$

where:

$\vec{V}(T)$  - is the vector of the speed of the fluid flow;

$\kappa$  - is the permeability of the medium; and

$\mu$  - is the fluid viscosity.

22 Once we have obtained a relative estimate of the total ground pressure  $P(T)$  for one of  
23 reflecting horizons using the seismic data, then we can employ a method for finding the  
24 parameters

25 →  
 26  $V(T)$ ,  $c$  and  $\mu$  using Equation (15) by making certain assumptions about the model

1 of the fracture-porous volume of the medium in the studied interval of the subsurface. The  
2 derived set of the fluid-dynamic parameters of the reservoir within an oil or gas field will reflect  
3 the dynamic state of the fluid mixture at the time of determination of these parameters.

4 Some general peculiarities of fluid migration and permeability in a discrete system are  
5 depicted in Fig. 6. Fig. 6 shows a simple and most general variant of a composition of three  
6 formation units 61, 62 and 63 of low level ( $B_L$ ), and each formation unit represents a layer  
7 composed of elementary blocks. It is supposed that the geometry and orientation of these blocks in  
8 layers can be arbitrary in the plane XY. In such a scheme the total permeability  $c_i$  of each layer  
9 will be determined by several main factors:

10 The average value of the blocks' void interval in a horizontal direction ( $m_v$ ).

11 The thickness of given layer ( $h$ ).

12 The permeability of each block in a layer (block or so-called matrix permeability). And,

13 The permeability of the upper and lower boundaries of a considered formation unit (boundary  
14 permeability or hydrodynamic contact along the horizontal boundaries of formation units in the  
15 context of discrete medium). This permeability is conditionally determined by the structure of a  
16 contact plane with the vertical "thickness"  $m_h$ .

17 In a generally accepted scheme of determination of true fracture permeability it is  
18 assumed that the block and fracture voids compose a common hydrodynamic system where the  
19 model of Darcy's flow is true. The permeability of a composition of layers with block structure  
20 in the normal (i.e., vertical) direction will be significantly lower than in a horizontal direction,  
21 since the value of void interval between the layers (horizontal contact of the blocks), which we  
22 notified as  $m_h$ , is always considerably less than  $m_v$ . Intersections of the sides of the blocks  
23 belonging to adjacent layers (in separate points such as the point S in Fig. 6) also cannot

1 significantly increase the vertical permeability of discrete rocks. Therefore, assuming some  
 2 general direction of fluid flow exists, the speed and direction of the flow  $\vec{V}$  will be different in  
 3 each considered layer. That is, discrete systems possess an evident anisotropy of the fluid flow  
 4 parameters, and consequently, the permeability in such systems is a tensor.

5 By analogy with a generally accepted representation of flow as a conductivity, we will  
 6 consider such a thin anisotropic layer and define the continuity equation for an incompressible  
 7 fluid with the viscosity  $\mu$  as the initial one

8  $\nabla \cdot \vec{V} = 0$  (Eqn. 16)

9 Then, let :

$$\vec{V} = \frac{\hat{c}}{\mu} \nabla P_d = \frac{\hat{c}}{\mu} \left( \frac{\partial P_d}{\partial x} \vec{i} + \frac{\partial P_d}{\partial y} \vec{j} \right) \quad (\text{Eqn. 17})$$

10 where  $\hat{c}$  is the permeability tensor in the main axes:

$$\hat{c} = \begin{vmatrix} c_{xx} & 0 \\ 0 & c_{yy} \end{vmatrix} \quad (\text{Eqn. 18})$$

11 Then from the continuity equation Eqn. (16):

$$\frac{\partial}{\partial x} \left( c_{xx} \frac{\partial P_d}{\partial x} \right) + \frac{\partial}{\partial y} \left( c_{yy} \frac{\partial P_d}{\partial y} \right) = c_{xx} \frac{\partial^2 P_d}{\partial x^2} + c_{yy} \frac{\partial^2 P_d}{\partial y^2} = 0 \quad (\text{Eqn. 19})$$

12 Next we introduce the coordinates:  $\xi = \frac{x}{\sqrt{c_{xx}}} ; \eta = \frac{y}{\sqrt{c_{yy}}}.$

13 Then:  $\frac{\partial^2 P_d}{\partial \xi^2} + \frac{\partial^2 P_d}{\partial \eta^2} = 0$ . This gives us:

1,0300 1

$$P_d = A \ln(\xi^2 + \eta^2) = A \ln\left(\frac{x^2}{c_{xx}} + \frac{y^2}{c_{yy}}\right) \quad (\text{Eqn. 20})$$

1,0301 2 The contours of equal pressure have the following form:

$$\frac{x^2}{c_{xx}} + \frac{y^2}{c_{yy}} = \text{const}$$

1,0302 3 and are the ellipses with the ratio of semi-axes:  $\frac{l^2}{c_{xx}} = \frac{c_{yy}}{c_{xx}}$

4 The constant  $A$  of Eqn. 20 we obtain from the expression:

1,0303 5

$$Q = \int_l D_n dl \quad (\text{Eqn. 21})$$

6 where  $l$  is the outline surrounding the region of the pressure source, and  $Q$  is flow rate of a fluid

7 from the deformed region of small size  $Dn$ . From this we obtain the following results:

1,0304 8

$$A = \frac{\mu Q}{4\pi \sqrt{c_{xx} c_{yy}}} \quad (\text{Eqn. 22})$$

9 and

10

$$P_d = -\frac{\mu Q}{4\pi \sqrt{c_{xx} c_{yy}}} \ln\left(\frac{x^2}{c_{xx}} + \frac{y^2}{c_{yy}}\right) \quad (\text{Eqn. 23})$$

11 and further:

12

$$V_x = -\frac{c_{xx}}{\mu} \frac{\partial P_d}{\partial x} = \frac{Q}{2\pi} \frac{1}{\sqrt{c_{xx} c_{yy}}} \frac{x}{\frac{x^2}{c_{xx}} + \frac{y^2}{c_{yy}}} \quad (\text{Eqn. 24})$$

13 and

14

$$V_y = -\frac{c_{yy}}{\mu} \frac{\partial P_d}{\partial y} = \frac{Q}{2\pi} \frac{1}{\sqrt{c_{xx} c_{yy}}} \frac{y}{\frac{x^2}{c_{xx}} + \frac{y^2}{c_{yy}}} \quad (\text{Eqn. 25})$$

T,0310

1 The vector of the flow speed  $\vec{V}$  is directed radially:  $\frac{V_{xx}}{V_{yy}} = \frac{x}{y}$ . Then we have:

T,0311

2

$$V_{x(y=0)} = \frac{1}{x} \frac{Q}{2\pi} \sqrt{\frac{c_{xx}}{c_{yy}}} \quad ; \quad V_{y(x=0)} = \frac{1}{y} \frac{Q}{2\pi} \sqrt{\frac{c_{yy}}{c_{xx}}} \quad (\text{Eqn. 26})$$

3 And for the circle  $x = y$  we have:

T,0312

4

$$\frac{V_{x(y=0)}}{V_{y(x=0)}} = \frac{c_{xx}}{c_{yy}} \quad (\text{Eqn. 27})$$

5 Thus, it follows that the regions of higher permeability coincide with the regions of higher fluid

T,0313

6 speeds. But the pressure gradients are equal at  $\varphi = 0$  ;  $\varphi = \frac{\pi}{2}$ :

T,0314

7

$$\frac{\partial P_d}{\partial x}(y=0) = -\frac{1}{x} \frac{\mu Q}{2\pi} \frac{1}{\sqrt{c_{xx} c_{yy}}} \quad (\text{Eqn. 28})$$

8 and

9

$$\frac{\partial P_d}{\partial y}(x=0) = -\frac{1}{y} \frac{\mu Q}{2\pi} \frac{1}{\sqrt{c_{xx} c_{yy}}} \quad (\text{Eqn. 29})$$

10 It is therefore accurate to say that the pressure gradients are maximum when  $\varphi = \frac{\pi}{4}$ . At

11 any other  $\varphi$  the pressure gradients have lower values. Therefore, the circle diagram 71 for the  
12 pressure gradients have a form shown in Fig. 7(a). At the same time, in the presence of triaxial  
13 anisotropy, as shown in Fig. 6, we have a circular graph 72 for a certain plane passing through  
14 two main directions as depicted in Fig. 7(b). As applied to the considered problem of fluid flow  
15 in a discrete medium, the above description indicates that a real formation unit in the form of a  
16 discrete layer is characterized with the anisotropy of permeability and the ability to deviate the

1 fluid flow from the initial direction and to change the rate of the fluid flow.

2 Next we consider the situation where the sources and drains of a fluid are formed in each  
3 unit volume of a discrete medium due to variation of the total voidness as a result of continuous  
4 change of the total ground pressure towards its increase (compression) or decrease  
5 (decompression). Then we have from the equation of continuity:

*T,0320* 6 
$$\frac{\partial}{\partial t}(Fr) + \nabla(rV) = 0 . \quad (\text{Eqn. 30})$$

7 For an incompressible fluid with a constant density  $\rho$  it follows that

*T,0321* 8 
$$\nabla V = -\frac{\partial F}{\partial t} = -q \quad (\text{Eqn. 31})$$

9 where  $V$  is the speed of Darcy's flow,  $F$  is the total voidness (fracture-porous volume), and  $q$  is  
10 the rate of its change (  $\text{c}^{-1}$  ). We will also accept that the rate of the volumetric deformation  
11  $\Delta D/\Delta t$  of a certain volume of the discrete medium  $D$  is related to the rate of change of the total  
12 voidness solely. That is:

*T,0322* 13 
$$q = \frac{\Delta D}{D\Delta t} \quad (\text{Eqn. 32})$$

14 By substituting the expression for the speed of Darcy's flow  $V=c/\mu \text{ grad } P_d$  in Eqn. (15), we  
15 obtain the Poisson's equation for pressure in the following form:

*T,0323* 16 
$$\nabla^2 P_d = -\frac{\mu}{c} \nabla \frac{c}{\mu} \nabla P_d + \frac{\mu}{c} q \quad (\text{Eqn. 33})$$

17 In the case of a medium with a constant permeability  $c_0$  and a homogeneous fluid with a  
18 viscosity  $\mu_0$ , we have:

*T,0324* 19 
$$\Delta P_d = -\frac{\mu_0 q}{c_0}$$

1 and 
$$P_0 = -\frac{\mu_0}{4\pi c_0} \int_{D_0} \frac{qdD_0}{R}$$
 (Eqn. 34)

2 where  $dD_0 = dx_0 dy_0 dz_0$  is the volume being deformed.

3 The expression for the pressure in the presence of a heterogeneous region  $D$ , in which  $c$   
4 and  $\mu$  are the function of coordinates, can be written as:

1,033\5

$$P_d = P_0 - \frac{1}{4\pi} \int_D \left( \frac{c\mu_0}{c_0\mu} - 1 \right) \nabla_D P_d \frac{\mathbf{r}}{r^3} dD \quad (\text{Eqn. 35})$$

6 where  $\mathbf{r} = (x-\xi)\mathbf{i} + (y-\eta)\mathbf{j} + (z-\zeta)\mathbf{k}$ , and  $dD = d\xi d\eta d\zeta$ .

7 Equations (34) and (35) can be directly generalized for the case of several deformed and  
8 heterogeneous regions, and the volumes  $D$  and  $D_0$  can coincide partially or completely. If we  
9 assume that a small deformation does not cause a considerable displacement of the permeability  
10 boundaries of considered volumes, there are several deformed volumes  $D_0 = \sum D_{0j}$ ,  
11  $j=1, 2, 3, \dots, n$ , and each volume  $D_{0j}$  is characterized with its own rate of volumetric deformation  
12  $q_j$ . The rate of volumetric deformation has different signs in the directions of compression and  
13 decompression of the volumes. Accordingly it is possible to construct the sedimentary cover in  
14 the form of considered model of a discrete dynamic system. In a given case the problem of a  
15 basin's dynamics is directly associated with the problem of variation of the medium permeability  
16 as a time function. This eventually leads to formation of absolutely natural communicating  
17 patterns of the blocks: one system of blocks squeezes the fluid out, while the other system of  
18 blocks absorbs it.

19 For regions sufficiently extensive along the axis OY in comparison with the dimensions  
20 along the other axes we can write the equation in two-dimensional case, similar to Equations (34)

1 and (35), in the form:

$$P_d = \frac{\mu_0}{2\pi c_0} \int q \ln R dS_0 - \frac{1}{2\pi} \int \left( \frac{c\mu_0}{c_0\mu} - 1 \right) \nabla_D P_d \frac{\mathbf{r}}{r^2} dS . \quad (\text{Eqn. 36})$$

3 The integral equation for the gradient of potential can be obtained for inner points of the cross-  
4 section  $S$  using Eqn. 36 as follows:

$$\nabla_A P_d = \frac{\mu_0}{2\pi c_0} \int q \frac{\mathbf{R}}{R^2} dS_0 - \frac{1}{2\pi} \nabla_A \int \left( \frac{c\mu_0}{c_0\mu} - 1 \right) \nabla_M P_d \frac{\mathbf{r}}{r^2} dS \quad (\text{Eqn. 37})$$

6 where:  $\nabla_A = \mathbf{i} \partial/\partial x + \mathbf{k} \partial/\partial z$ ,  $\nabla_D = \mathbf{i} \partial/\partial \zeta + \mathbf{k} \partial/\partial \zeta$ ,  $dS = d\xi \partial \zeta$ ,  $\mathbf{R} = (x - x_0)\mathbf{i} + (z - z_0)\mathbf{k}$ ,

7  $\mathbf{r} = (x - \xi)\mathbf{i} + (z - \zeta)\mathbf{k}$ , and  $dS_0 = dx_0 dz_0$ .

8 By solving the integral Equation (37) we can determine the pressure from Eqn. (36) using

9 the same matrix of inner values  $\nabla_D P_d$ .

10 Now we will consider a thin horizontal layer located in a medium impermeable for a  
11 fluid. We will also superpose the regions of deformation and heterogeneity  $S$  and  $S_0$ . In this case  
12 Equations (36) and (37) should be written in the form

$$P_d = \frac{1}{2\pi} \int \frac{\mu_0}{c_0} q \ln R dS - \frac{1}{2\pi} \int \left( \frac{c\mu_0}{c_0\mu} - 1 \right) \nabla_M P_d \frac{\mathbf{r}}{r^2} dS \quad (\text{Eqn. 38})$$

13 and  $\nabla_A P_d = \frac{1}{2\pi} \int \frac{\mu_0}{c_0} q \frac{\mathbf{r}}{r^2} dS - \frac{1}{2\pi} \nabla_A \int \left( \frac{c\mu_0}{c_0\mu} - 1 \right) \nabla_M P_d \frac{\mathbf{r}}{r^2} dS \quad (\text{Eqn. 39})$

14 where  $\nabla_A = \mathbf{i} \partial/\partial x + \mathbf{j} \partial/\partial y$ ,  $\nabla_M = \mathbf{i} \partial/\partial \zeta + \mathbf{j} \partial/\partial \eta$ ,  $dS = d\xi \partial \eta$ , and  $\mathbf{r} = (x - \xi)\mathbf{i} + (y - \eta)\mathbf{k}$ .

15 After scalarization the vector integral Equation (39) can be considered as a system of  
16 integral equations of Fredholm of the second type, if the distribution  $c/\mu$  is known and the  
17 pressure gradient should be calculated, as well as the equation of Fredholm of the first type for an

1 unknown distribution  $c/\mu$ , if the distribution of the pressure gradient is specified. If the main  
2 target is evaluation of the correspondence between the pressure and the permeability, then it is  
3 proper to solve the direct problem of determining the pressure gradient on given distribution of  
4 the permeability by using Eqn. (39) as the Fredholm equation of the second type, and then to  
5 calculate the pressure using Eqn. (38).

6 From the practical point of view the general scheme of determination of the main fluid-  
7 dynamic parameters can be presented with the aid of a diagram shown in Fig. 8. With reference  
8 to Fig. 8, the initial information used to obtain a solution to the problem is the relative  
9 distribution of over-hydrostatic pressure  $P_d$  81, which can be determined from the seismic  
10 attributes from the studied interval of a seismic section (2D-3D) 85 in the manner described in  
11 the first part of the above Detailed Description. Then, by solving Equation (39) with respect to an  
12 unknown distribution  $c/\mu$ , we can will derive  $c$  82 in the same points and coordinates of the  
13 seismic section for a specified  $\mu$  (for example,  $\mu=1$ ). An alternative solution at this step can be  
14 obtained by specifying  $c/\mu$  from geological data, if the location of the stratigraphic boundaries  
15 is known and the properties of rocks are determined on well data 83. At the final stage 84 the  
16 components  $Vx$  and  $Vy$  of the vector of fluid flow speed are derived in correspondence with the  
17 ratios from Eqn. (26) using known distributions  $P_d$  and  $c/\mu$ . In given example the method  
18 supposes determination of the fluid-dynamic parameters on one seismic section and construction  
19 of a map in vertical plane (x – the direction of the seismic section; y - the vertical axis of time or  
20 depth). The same can be done for many seismic sections (i.e., a three-dimensional or 3D  
21 solution), and in this case horizon-oriented maps of target parameters are created for specified  
22 depths. The derived set of the fluid-dynamic parameters of the reservoir within an oil or gas field  
23 will reflect the dynamic state of fluid mixture at the time of determination of these parameters.

1        This method thus allows for the following information to be obtained:

2        1. To locate the regions with highest permeability within a reservoir, or the regions with  
3        anomalous deviations of the vector of fluid flow speed from the dominant direction. In  
4        both cases such regions can testify to the presence of hydrocarbon traps.

5        2. To delineate more accurately an oil or gas accumulation within the limits of given  
6        reservoir.

7        3. To determine the discrepancy between the new and the previous outlines of the  
8        accumulation in the case where its spatial location was known from the results of the  
9        previous investigations (seismic or other methods).

10       4. To optimally design the trajectory of the wellbore. This is of particular advantage for  
11       horizontal drilling since the highest productivity will be obtained in the situation where  
12       the axis of the wellbore is located at a certain angle to the direction of the maximum  
13       permeability  $C$ , which is a tensor value in dynamic systems. And,

14       5. To optimally plan the development scheme for given field with account for the current  
15       and the future dynamics of the fluid mixture.

16       While the above invention has been described in language more or less specific as to  
17       structural and methodical features, it is to be understood, however, that the invention is not  
18       limited to the specific features shown and described, since the means herein disclosed comprise  
19       preferred forms of putting the invention into effect. The invention is, therefore, claimed in any of  
20       its forms or modifications within the proper scope of the appended claims appropriately  
21       interpreted in accordance with the doctrine of equivalents.